Available online at www.sciencedirect.com
SCIENCE DIRECT®
Journal of Solid State Chemistry 177 (2004) 3324–3332
JOURNAL OF SOLID STATE CHEMISTRY
http://elsevier.com/locate/jssc

Local structure and hyperfine interactions of ^{57}Fe and ^{119}Sn atoms in brownmillerite-like ferrite $Sr_2Fe_{1.98}Sn_{0.02}O_{5+x}$

Igor Presniakov,[a] Alexey Sobolev,[a] Konstantin Pokholok,[a] Gérard M. Demazeau,[b,*] and Alexey Baranov[c]

[a] Department of Chemistry, Lomonosov Moscow State University, 119992 Leninskie Gory, Moscow, Russia
[b] Institut de la Chimie de la Matière Condensée de Bordeaux (ICMCB), Universite Bordeaux 1 et CNRS 9048, France
[c] Faculty of Materials Science, Lomonosov Moscow State University, 119992 Leninskie Gory, Moscow, Russia

Received 10 March 2004; received in revised form 24 May 2004; accepted 25 May 2004

Available online 20 July 2004

Abstract

Mössbauer spectroscopy has been applied for studying local environment of ^{57}Fe and ^{119}Sn probe atoms within tin-doped $Sr_2Fe_{1.98}Sn_{0.02}O_{5+x}$ ($x \leqslant 0.02$) ferrite with the brownmillerite-type structure. ^{57}Fe Mössbauer spectra indicate no appreciable local distortions induced by the tin dopant atoms. The ^{119}Sn spectra recorded below the magnetic ordering temperature (T_N) can be described as a superposition of two Zeeman sextets, which indicate that Sn^{4+} dopant ions are located in two non-equivalent crystallographic and magnetic sites. The observed hyperfine parameters were discussed supposing Sn^{4+} cations to replace iron cations in the octahedral (Sn_O) and tetrahedral (Sn_T) sublattices. It has been supposed that Sn^{4+} cations being stabilized in the tetrahedral sublattice complete their nearest anion surrounding up to the octahedral oxygen coordination "Sn_T^{4+}". Annealing of the $Sr_2Fe_{1.98}Sn_{0.02}O_{5+x}$ in helium flux conditions at 950°C leads to formation of divalent Sn^{2+} cations with a simultaneous decrease of the contribution for the Sn_T^{4+} sub-spectrum. The parameters of combined electric and magnetic hyperfine interactions of the $^{119}Sn^{2+}$ sub-spectrum underline that impurity atoms are stabilized in the sp^3d-hybrid state in the oxygen distorted tetragonal pyramid. The analysis of the ^{119}Sn spectra indicates a chemical reversibility of the processes $Sn_T^{2+} \rightleftharpoons Sn_T^{4+}$ within the tetrahedral sublattice of the brownmillerite-type ferrite.

Keywords: Iron oxides; Probe atoms; Mössbauer spectroscopy; Local structure; Hyperfine interactions

1. Introduction

The perovskite-like ferrites $AFeO_{3-\gamma}$ (A = Ca, Sr, Ba) are of considerable interest due to their ability to accommodate a large concentration of anion vacancies, and γ can take values in the range $0 \leqslant \gamma \leqslant 0.5$ [1]. The oxygen non-stoichiometry depends on the ability of iron to exist as both Fe^{4+}, in the fully oxidized ferrates $AFeO_3$ ($\gamma = 0$), and Fe^{3+} in the fully reduced ferrites $AFeO_{2.5}$ ($\gamma = 0.5$). Compositions with $0 < \gamma < 0.5$ can be regarded as mixed-valence compounds in which both Fe^{3+} and Fe^{4+} cations are present. The oxygen vacancies and mixed valence states of iron give rise to the high ionic and electronic conductivities of these compounds, which are essential for potential applications, e.g., as ceramic membranes for oxygen separation [2], electrodes of solid oxide fuel cells [3], and sensors [4] for various gases including H_2, CO, CO_2, CH_4.

Among known oxygen-deficient ferrites the highest oxygen ionic conductivity was observed in compounds based on strontium $SrFeO_{3-\gamma}$ ferrites [5]. It has been shown that substitution of Fe^{3+} for higher valence diamagnetic metal cations, such as Sn^{4+}, Ti^{4+}, Zr^{4+}, increases the oxygen ionic transport [6–8]. This effect can be associated with a possible stabilization of the cubic perovskite structure, which provides better geometrical abilities for hopping of oxygen vacancies and electrons in comparison with various ordered perovskite-like phases. Several studies concerning the nature of oxygen vacancies in the disordered region of the systems

*Corresponding author. Fax: +33-5-40-00-27-10.
E-mail addresses: alex@radio.chem.msu.ru (I. Presniakov), demazeau@icmcb.u-bordeaux.fr (G.M. Demazeau).

0022-4596/$ - see front matter © 2004 Elsevier Inc. All rights reserved.
doi:10.1016/j.jssc.2004.05.048

$SrFe_{1-x}Sn_xO_{3-\gamma}$ [9–11] and $SrFe_{1-x}Ti_xO_{3-\gamma}$ [12] were reported. The ^{57}Fe Mössbauer spectroscopy, which is one of the most effective tools for such studies, has showed that iron ions are located in octahedral (Fe_O), tetrahedral (Fe_T) and pentacoordinated (Fe_P) sites. Subsequent ^{57}Fe Mössbauer investigations of $SrFe_{1-x}Ti_xO_{3-\gamma}$ [13] system revealed that a small number of the Ti atoms are located on non-octahedral sites, the relative proportion of which decreases with increasing concentration of oxygen vacancies. However, detailed information concerning the local structure of diamagnetic cations is absent.

In this paper, we report the results of ^{57}Fe and ^{119}Sn Mössbauer study of tin-substituted ferrite $Sr_2Fe_{1.98}Sn_{0.02}O_{5+x}$ ($x \approx 0$) synthesized over a range of annealing temperatures and oxygen partial pressure. The oxygen-ordered end-member phase $SrFeO_{2.5}$ ($\gamma = 0.5$) possesses a brownmillerite-type structure which is derived from the other end-member cubic $SrFeO_3$ ($\gamma = 0$) perovskite structure by creating rows of oxygen vacancies along the $[101]_p$ direction in every other $(010)_p$ plane. The resulting structure contains alternating layers of octahedral (FeO_6) and tetrahedral (FeO_4) perpendicular to the *b*-axis (Fig. 1). Such structure is favored by the possibility to accommodate trivalent iron in both octahedral and tetrahedral sites.

Recently we synthesized and characterized by ^{119}Sn probe Mössbauer Spectroscopy the ferrite $Ca_2Fe_{1.98}Sn_{0.02}O_5$ [14,15] with the aim of exploring how the local structure of the parent compound $Ca_2Fe_2O_5$ changes when the Fe^{3+} ions are replaced by diamagnetic tin atoms. It was shown that the Sn^{4+} dopant cations occupy only octahedral cationic positions in brownmillerite-type structure of $Ca_2Fe_2O_5$. The comparative study of ^{119}Sn and ^{57}Fe Mössbauer spectra indicated no appreciable local distortions of the $Ca_2Fe_2O_5$ lattice induced by the tin dopant atoms.

Here we focus our attention on relationship between local structure and hyperfine parameters of ^{119}Sn diamagnetic atoms in the antiferromagnetic region, $T < T_N$, of the $Sr_2Fe_{1.98}Sn_{0.02}O_5$. In the case of magnetically ordered matrices, the ^{119}Sn Mössbauer spectra exhibit Zeeman splitting due to the spin polarization of the diamagnetic probe by its magnetic neighbors [16]. The magnetic information obtained from such spectra can be of great importance for the cationic environment of the ^{119}Sn probe atoms to be determined.

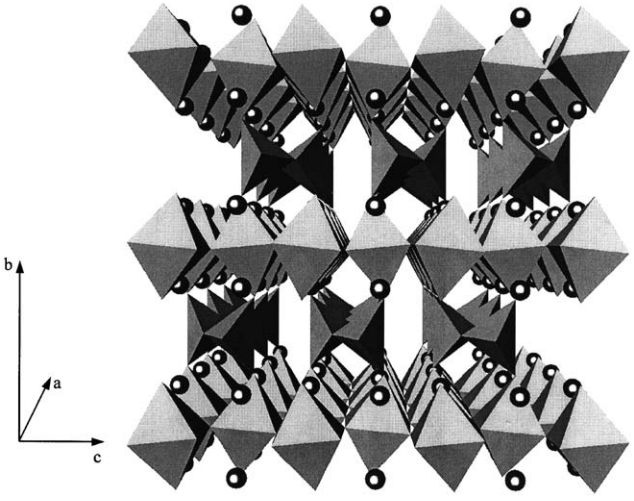

Fig. 1. Schematic representation of the $Sr_2Fe_2O_5$ brownmillerite-type structure with I_{2mb} crystal symmetry.

2. Preparation and characterization

The $Sr_2Fe_{1.98}Sn_{0.02}O_5$ polycrystalline sample was prepared in three steps. The first one involved the preparation of the precursor $Fe_{1.98}Sn_{0.02}O_3$. At this step iron (III) and tin (IV) hydroxides were coprecipitated from an acid solution of Fe^{3+} and Sn^{4+} stoichiometric mixture chlorides. The homogeneous hydroxide mixture was washed, dried and annealed in air at 900°C until the formation of the ^{119}Sn doped $Fe_{1.98}Sn_{0.02}O_3$ oxide:

$$Fe^{3+}_{(aq)} + {}^{119}Sn^{4+}_{(aq)} \xrightarrow{NH_3\cdot H_2O} Fe_{0.99}Sn_{0.01}(OH)_3 \xrightarrow{900^\circ C} Fe_{1.98}Sn_{0.02}O_3$$

At the second step, weighed amounts of spectroscopic grade $SrCO_3$ and $Fe_{1.98}Sn_{0.02}O_3$ in the stoichiometric ratio were ground together in ball mill, pressed into a pellet and fired in air ($P_{O2} = 2 \cdot 10^4$ Pa) at 1300°C for 3 days with two intermediate grindings before quenching onto a metal plate in air:

$$Fe_{1.98}Sn_{0.02}O_3 + SrCO_3 \xrightarrow{1300^0C} Sr_2Fe_{1.98}Sn_{0.02}O_{5.72}$$

Stoichiometric strontium ferrite (without the oxygen excess) was obtained in the third step by reduction at 1000°C under dynamic vacuum ($P_{O2} = 1$ Pa):

$$Sr_2Fe_{1.98}Sn_{0.02}O_{5.72} \xrightarrow{P_{O_2}=1\ Pa,\ 850^\circ C} Sr_2Fe_{1.98}Sn_{0.02}O_{5+x}\ (x \approx 0)$$

The oxygen stoichiometry which is related to Fe^{4+}/Fe^{3+} proportion was determined by means of cerimetry [17]: 20–30 mg of the sample was dissolved in a standardized solution of ammonium iron (II) sulfate, followed by the addition of distilled HCl and a titration with cerium (IV) sulfate using ferroin indicator. The chemical analysis confirmed the absence within experimental error of Fe^{4+} cations, i.e., the $Sr_2Fe_{1.98}Sn_{0.02}O_{5.02\pm0.01}$ composition (further designated as $Sr_2Fe_{1.98}Sn_{0.02}O_5$).

Powder X-ray diffraction data were measured with a Siemens diffractometer using Cu$K\alpha$ radiation. The

X-ray pattern was indexed on the basis of the orthorhombic cell. The indexation was in agreement with the space group *I2mb* (C_{2v}^{22}) previously determined by neutron powder diffraction on the $Sr_2Fe_2O_5$ ferrite [18].

Mössbauer spectra were measured in transmission mode using a conventional constant acceleration spectrometer. The radiation sources $Ca^{119m}SnO_3$ and $^{57}Co(Rh)$ were kept at room temperature. All isomer shifts refer to the $CaSnO_3$ and α-Fe absorbers at 300 K. The values for the hyperfine magnetic fields (H) at ^{119}Sn nuclei were obtained using values of 23.871 keV for the γ-ray energy, $\mu_g = -1.0461$ nuclear magnetons for the ground-state magnetic moment.

3. Results

3.1. ^{57}Fe Mössbauer spectra

The ^{57}Fe spectrum of substituted $Sr_2Fe_{1.98}Sn_{0.02}O_5$ ferrite at 80 K consists of two magnetic Zeeman sextets (Fig. 2). The isomer shifts ($\delta_1 = 0.48 \pm 0.01$ mm/s; $\delta_2 = 0.32 \pm 0.01$ mm/s) and hyperfine magnetic fields ($H_1 = 540 \pm 1$ kOe; $H_2 = 452 \pm 1$ kOe) of these sextets correspond to the trivalent iron cations in octahedral (Fe_O^{3+}) and tetrahedral (Fe_T^{3+}) oxygen environments [19,20]. The smaller $\delta(Fe_T)$ and $H(Fe_T)$ values as compared to those for Fe_O^{3+} cations are caused by a greater covalence of the Fe_T^{3+}–O chemical bonds and, hence, by a greater population of the valence 4*s*-orbitals for these cations [21]. The ratio of the areas corresponding to the sextets, $A(Fe_O)/A(Fe_T) = 0.97$, is close to unity which is consistent with equal populations of the octahedral and tetrahedral iron positions in the brownmillerite-type structure. It should be noted, that the content of tin probe atoms in $Sr_2Fe_{1.98}Sn_{0.02}O_5$ is very small (~1 at%) and it does not introduce any significant changes of the spectral contribution values of each sextet as compared to those for unsubstituted $Sr_2Fe_2O_5$ ferrite.

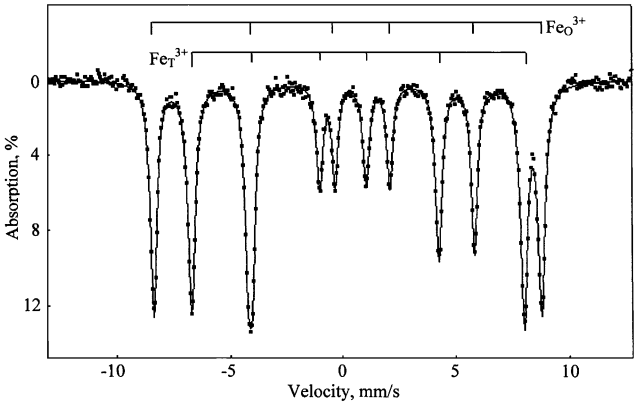

Fig. 2. ^{57}Fe Mössbauer spectrum of $Sr_2Fe_{1.98}Sn_{0.02}O_5$ recorded at 80 K.

At $T \ll T_N$, the main line splitting of Zeeman hyperfine structure at Fe^{3+} nuclei is caused by magnetic dipole interactions. In this case the quadrupole shift (ε) in the line positions of Zeeman sextets due to the quadrupole interactions is treated as a perturbation and is defined by the following equation [22]:

$$\varepsilon = eQ_{3/2}V_{zz}(3\cos^2\theta - 1)/8, \quad (1)$$

where $Q_{3/2}(>0)$ is the nuclear quadrupole moment of the first excited state of ^{57}Fe nuclei and θ is the angle between the directions of the principal component, V_{zz}, of the electric field gradient (EFG) tensor and the hyperfine field $H(Fe^{3+})$.

The analysis of the spectrum shows that ε value is negative for Fe_O^{3+} sites and positive for Fe_T^{3+} sites. As the magnetizations of both $M(Fe_O)$ and $M(Fe_T)$ sublattices, which are collinear with the hyperfine fields $H(Fe_O)$ and $H(Fe_T)$, are directed along *a*-axis of the orthorhombic ferrit cell (namely $\theta = 90°$) this leads to the conclusion that $V_{zz}(Fe_O) > 0$ and $V_{zz}(Fe_T) < 0$, respectively. This result is in accordance with the local crystallographic structure of $Sr_2Fe_2O_5$ (Fig. 3). Indeed, since the Fe^{3+}:$3d^5$ cations in high spin state have isotropic electronic configuration, the main component of EFG observed at iron nuclei is due to the distortion of their crystallographic surroundings (lattice contribution, V_{zz}^L). In the brownmillerite-type structure,

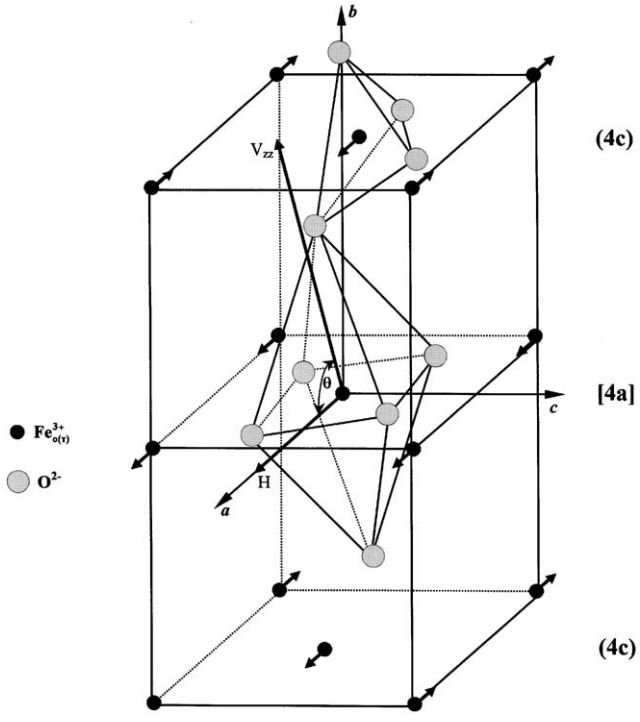

Fig. 3. Idealized fragment of the iron local environment in $Sr_2Fe_2O_5$ structure.

tetragonally distorted octahedral (FeO_6) and tetrahedral (FeO_4) polyhedra are elongated ($V_{zz}^{L}>0$) and compressed ($V_{zz}^{L}<0$), respectively, along the local four-fold *b*-axis, which is nearly coincident with the direction of the V_{zz}^{L} on the Fe_O^{3+} and Fe_T^{3+} sites (Fig. 3).

3.2. ^{119}Sn Mössbauer spectra

The ^{119}Sn Mössbauer spectrum of $Sr_2Fe_{1.98}Sn_{0.02}O_5$ recorded above $T>T_N\approx715$ K [18] (Fig. 4a) can be described as a superposition of two Sn(1) and Sn(2) quadrupole doublets with different quadrupole splittings, Δ, which indicate that dopant tin ions are located in two non-equivalent crystallographic sites. The Δ_1 and Δ_2 values are large (Table 1), showing the low local symmetry of both tin sites in the ferrite structure. Since the lattice component, V_{zz}^{L}, at the nuclei of spherically symmetric cations Sn^{4+}:$4d^{10}5s^0$ is temperature independent, we used the absolute values of the quadrupole coupling constants, $|eQ_{3/2}V_{zz}^{L}(i)|=2\Delta_{(i)}$ $(i=1,\ 2)$, determined at $T>T_N$, for analysis the magnetically split spectra ($T<T_N$).

Below the magnetic ordering temperature, $T<T_N$, the ^{119}Sn spectrum is resolved into two magnetic Zeeman sextets (Fig. 4b). The isomer shift values for both sextets exhibit the usual increase, with respect to those at $T>T_N$ (Table 1), due to the second-order Doppler shift [23]. The observed δ values are consistent with tetravalent Sn^{4+} probe cations in other magnetically ordered oxides of transition metals [14,16,24–29]. The small paramagnetic component in the range of zero velocities can be related to tin atoms not incorporated in the ferrite structure and segregated as impurity oxygen phase, which was not detected in the X-ray data.

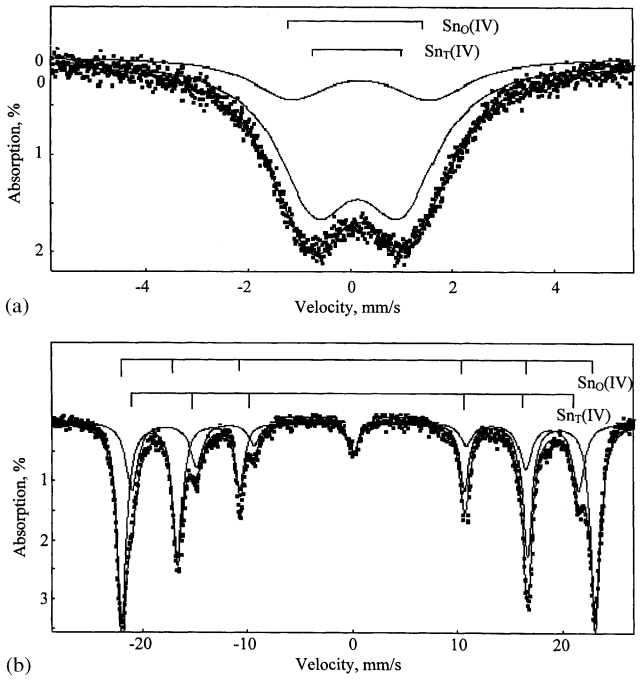

Fig. 4. ^{119}Sn Mössbauer spectra of $Sr_2Fe_{1.98}Sn_{0.02}O_5$ recorded at 800 K (a) and 80 K (b).

4. Discussion

The both Zeeman sextets in the ^{119}Sn Mössbauer spectra clearly demonstrate the existence of combined magnetic and quadrupole interactions, which is in agreement with the significant quadrupole splittings of Sn(1) and Sn(2) sub-spectra at $T>T_N$ (Fig. 4a). The experimental results show that quadrupole perturbation parameter ε (see Eq. (1)) is positive for the Sn(1) sites and negative for the Sn(2) sites. Taking into account that the *H* direction at ^{119}Sn probe atoms coincides with the direction of the magnetic moments of the neighboring iron cations [16], the $\theta\approx90°$ value corresponding to both Sn(1) and Sn(2) sites is consistent with local magnetic structure of $Sr_2Fe_2O_5$ [18] (Fig. 3). This assumption is based on the earlier conclusion [14,15] that tin probe atoms, being stabilized in the ferrite lattice, do not introduce any significant perturbation of its local magnetic structure. As $Q_{3/2}$ of the first excited state of ^{119}Sn is negative and the angular coefficient in Eq. (1), $3\cos^2(90°)-1$, positive, we concluded on the basis of the Fe^{3+} Mössbauer Spectra that V_{zz}^{L} value is positive on the Sn(1) sites and negative on the Sn(2) sites.

The positive sign for $V_{zz(1)}^{L}$ coincides with that for V_{zz}^{L} of the sole Zeeman structure of $^{119}Sn^{4+}$ probe cations in earlier studied $Ca_2Fe_{1.98}Sn_{0.02}O_{5m}$ [14,15]. This allowed

Table 1
^{119}Sn Mössbauer parameters of $Sr_2Fe_{1.98}Sn_{0.02}O_5$

T (K)	Site	δ (mm/s) ±0.01	Δ (mm/s) ±0.01	H (kOe)±1	θ (deg)±2	A (%)±1
800						
($T>T_N$)	Sn$_O$(IV)	0.06	0.84	—	—	79
	Sn$_T$(IV)	0.24	1.37	—	—	21
80						
($T<T_N$)	Sn$_O$(IV)	0.20	−0.84	372	86	78
	Sn$_T$(IV)	0.39	1.37	360	90	22

us to relate the Zeeman structure with the greater hyperfine field (H_1) to Sn_O^{4+} cations substituting Fe_O^{3+} cations in the octahedral sublattice of $Sr_2Fe_{1.98}Sn_{0.02}O_5$ structure. The opposite sign for $V_{zz(2)}^L$ (<0) of the second Zeeman sextet suggests that Sn(2) cations (further designated as Sn_T^{4+}) are localized in the tetrahedral sublattice of the brownmillerite-type ferrite. The above conclusions are in accordance with signs of the lattice contribution, V_{zz}^L, on Fe_O^{3+} ($V_{zz}^L>0$) and Fe_T^{3+} ($V_{zz}^L<0$) sites.

In a second part of such a discussion, the comparison of the H and δ values for Sn_O^{4+} and Sn_T^{4+} cations can bring some information concerning the local surrounding for both Sn^{4+} sites in the brownmillerite-type structure.

It is well known that Sn^{4+} cations always occupy sites exclusively with octahedral oxygen coordination in all the proper oxide phases. There are only two examples of oxide compounds for which the tetrahedral oxygen coordination for Sn^{4+} ions was assumed on the basis of Mössbauer spectra: $Ca_3Sn_3Ga_2O_{12}$ [30] and $Ca_3In_2Ge_{3-x}Sn_xO_{12}$ [31]. For both compounds having the garnet-type structure the Mössbauer spectra of tetrahedrally coordinated Sn^{4+} cations are characterized by high average value of isomer shifts, $\delta\approx0.86$ mm/s, which is in agreement with the increased covalence of shortened Sn–O bonds in the tetrahedral oxygen (SnO_4) polyhedra. However, in the case of $Sr_2Fe_{1.98}Sn_{0.02}O_5$, the isomer shift corresponding to Sn_T^{4+} cations is much smaller (see Table 1).

Furthermore, if Sn_T^{4+} cations were located in the tetrahedral oxygen polyhedra, the number of superexchange Sn_T–O–$Fe_{O,T}$ bonds, through which the hyperfine field $H(Sn_T)$ is induced at tin nuclei, would be fewer by two than in the case of Sn_O^{4+} cations localized in the octahedral sublattice of the same ferrite structure. In our previous work dealing with ^{119}Sn-doped $Ca_2Fe_{2-x}Sc_xO_5$ solid solutions it had been shown that partial contributions to $H(^{119}Sn)$ from each paramagnetic neighboring $Fe_{O,T}^{3+}$ cations were 50–60 kOe on the average [32]. Therefore, the absence of two Sn_T–O–Fe_T bonds should lead to a decrease of $H(^{119}Sn)$ value by 100–120 kOe. Actually, according to the data of Table 1, the hyperfine field at Sn_T^{4+} nuclei is weaker by 12 kOe than the corresponding value for Sn_O^{4+} cations.

Thus, on the basis of the above experimental data, it is possible to suppose that Sn_T^{4+} impurity cations, stabilized in the tetrahedral sublattice of $Sr_2Fe_{1.98}Sn_{0.02}O_5$, through oxygen diffusion complete their nearest anion surrounding up to the octahedral oxygen coordination, which appears to be most typical of tetravalent tin atoms. As a result Sn_T^{4+} cations become bound with six neighboring paramagnetic iron cations: $\{4Fe_T^{3+}+2Fe_O^{3+}\}$. This explains, in particular, the closeness of hyperfine fields $H(Sn_T)$ and $H(Sn_O)$ (Sn_O^{4+} cations also have six nearest paramagnetic neighbors: $\{4Fe_O^{3+}+2Fe_T^{3+}\}$).

We should pay attention to the unusual correlation of δ and H values for the "Sn_T^{4+}" ("Sn_T^{4+}" indicates that such a Sn^{4+} is located in the brownmillerite sublattice of tetrahedral sites but with a local pseudo-octahedral surrounding) and Sn_O^{4+} tetravalent tin cations in the $Sr_2Fe_{1.98}Sn_{0.02}O_5$ ferrite structure (see Table 1): the greater isomer shift (δ_2) corresponds to the weaker hyperfine field (H_2). Usually, an increase of the isomer shift for Sn^{4+} impurity cations in the magnetically ordered materials leads to an increase of the magnetic hyperfine field induced at their nuclei. This correlation may be explained by the increase of the covalence of the Sn–O bonds (δ increase) and, hence, an increase of the spin transfer degree in $Fe^{3+}\rightarrow O\rightarrow Sn^{4+}$ chains (H increase). In the case of $Sr_2Fe_{1.98}Sn_{0.02}O_5$, a higher covalence of Sn_T–O bonds (higher δ_2) is due to the fact that octahedral polyhedra "Sn_TO_6", formed from small tetrahedral polyhedra of unsubstituted ferrite, should have a smaller volume than normal octahedral interstices occupied by Sn_O^{4+} cations (smaller δ_1). However, the hyperfine field at diamagnetic ion nuclei depends not only on the Sn(Fe)–O bond covalence degree, but is also controlled by the angle φ in the Sn-O–Fe chains [16]. Notwithstanding the fact that the number of indirect $Sn_{O,T}$–O–Fe interactions is identical for both Sn_O^{4+} and "Sn_T^{4+}" sites, the average angle $\langle\varphi\rangle$ in these bonds significantly decreases when passing from (Sn_OO_6) polyhedra ($\langle\varphi\rangle_{Sn-O-Fe}=167^\circ$) to ($Sn_TO_6$) polyhedra ($\langle\varphi\rangle_{Sn-O-Fe}=136^\circ$) [18]. This eventually leads to the $H(Sn_O)$ decrease observed in the spectra, in comparison with $H(Sn_T)$.

The third part of this discussion is devoted to the study of the different behavior of Sn^{4+} impurity ions in isostructural $Sr_2Fe_{1.98}Sn_{0.02}O_5$ and $Ca_2Fe_{1.98}Sn_{0.02}O_5$ ferrites.

If we compare the behavior of ^{119}Sn probe atoms in $Sr_2Fe_{1.98}Sn_{0.02}O_5$ and early investigated tin-doped ferrite $Ca_2Fe_{1.98}Sn_{0.02}O_5$ [14,15] where Sn_O^{4+} cations occupy only positions in octahedral sublattice; one of the most probable causes of the different behavior of Sn^{4+} impurity cations in the two isostructural ferrites can be related to different mechanisms of phase formation in these compounds. The formation of stoichiometric dicalcium ferrite doped by ^{119}Sn is completed as early as at the first step including annealing ($P_{O2}=2\times10^4$ Pa) of $Fe_{1.98}Sn_{0.02}O_3$ and $CaCO_3$. In contrast, to achieve the required oxygen stoichiometry of $Sr_2Fe_{1.98}Sn_{0.02}O_5$, the ferrite $Sr_2Fe_{1.98}Sn_{0.02}O_{5.72}$ with the oxygen excess formed at the second stage should be annealed at a low partial pressure of oxygen. The $Sr_2Fe_2O_{5.72}$ structure was shown [33] to represent two cationic sublattice alternating along crystallographic direction (101), in the first of one Fe^{IV} cations occupy the sites with octahedral oxygen coordination (Fig. 5a). In the second sublattice

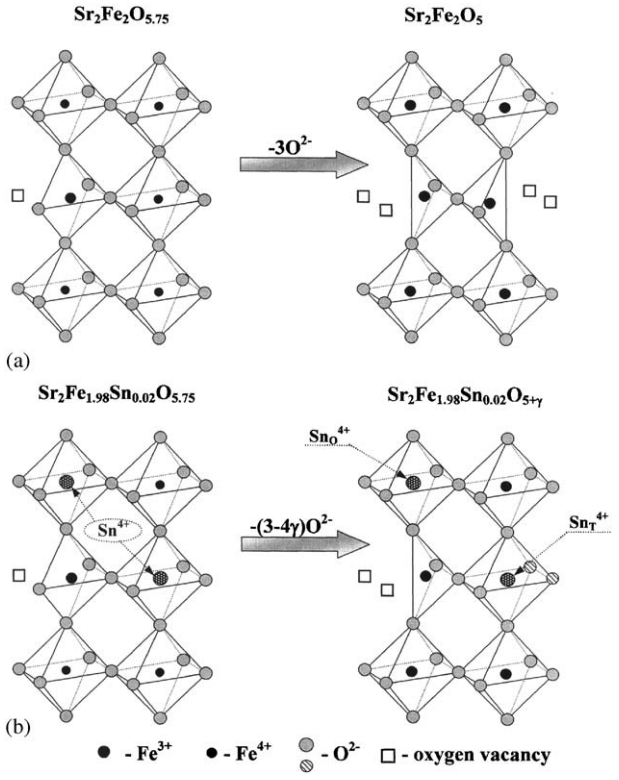

Fig. 5. Schematic representation of the structure evolution in $Sr_2Fe_2O_{5.75} \rightarrow Sr_2Fe_2O_5$ (a), and $Sr_2Fe_{1.98}Sn_{0.02}O_{5.75} \rightarrow Sr_2Fe_{1.98}Sn_{0.02}O_5$ (b) processes.

of this ferrite half of all the populating iron cations are also tetravalent in the octahedral oxygen surrounding. The other part is stabilized in the trivalent state with the anion surrounding corresponding to the tetragonal pyramid.

It may be assumed that impurity Sn^{4+} cations are distributed over both sublattices at the stage of $Sr_2Fe_{1.98}Sn_{0.02}O_{5.72}$ formation, statistically replacing isovalent Fe^{IV} cations with the octahedral oxygen coordination (Fig. 5b). In this case, two-thirds of all impurity Sn^{4+} cations should be in the first sublattice, and the other one-third in the second one. Reduction annealing of $Sr_2Fe_{1.98}Sn_{0.02}O_{5.72}$ at the second stage removes a fraction of oxygen atoms from the second sublattice, which is accompanied by transformation of anionic polyhedra with the octahedron symmetry and the tetragonal pyramid into tetrahedral polyhedra (Fig. 5a). However, taking into account the high affinity of Sn^{4+} cations to oxygen, one can assume that even those stabilized in the tetrahedral sublattice will preserve the octahedral oxygen neighborhood after reduction annealing in vacuum (Fig. 5b). As a result, two Zeeman splitting structures with the ratio of areas $A(Sn_O)/A(Sn_T) \approx 2$ will be observed in the ^{119}Sn spectrum of $Sr_2Fe_{1.98}Sn_{0.02}O_5$ ferrite produced at the last stage of the synthesis.

4.1. Stabilization of Sn^{2+} in brownmillerite-type structure

To confirm the conclusion that the second Zeeman structure can be related to octahedrally coordinated "Sn_T^{4+}" cations stabilized in the tetrahedral sublattice of the brownmillerite-type ferrite, the $Sr_2Fe_{1.98}Sn_{0.02}O_5$ sample was annealed at 950°C in a flux of $He + 2\%H_2$ ($P_{O2} \leqslant 10^{-15}$ Pa), which provides "harder" reduction conditions. The ^{57}Fe Mössbauer spectrum of the produced sample exhibited no appreciable changes in comparison with the spectrum of the same sample before the reduction annealing.

On the contrary, apart from the two sextets corresponding to the "Sn_T^{4+}" and Sn_O^{4+} cations, additional absorption arises in the ^{119}Sn spectrum of the reduced sample in the range of low velocities (Fig. 6a). One can see from Table 2 that the relative contribution (A) of the sextet corresponding to Sn_O^{4+} cations before and after reduction remains virtually unchanged, while the contribution of the sextet of the "Sn_T^{4+}" cations significantly decreases due to the emerging third form of tin impurity ions. This result allows an assumption that ferrite annealing under "hard" reduction conditions removes oxygen from the nearest anion environment of a fraction of the "Sn_T^{4+}" cations with formation of a new tin cation form with a decreased oxygen coordination number in the tetrahedral sublattice.

To determine the parameters of the spectrum corresponding to the new form of tin cations, measurements

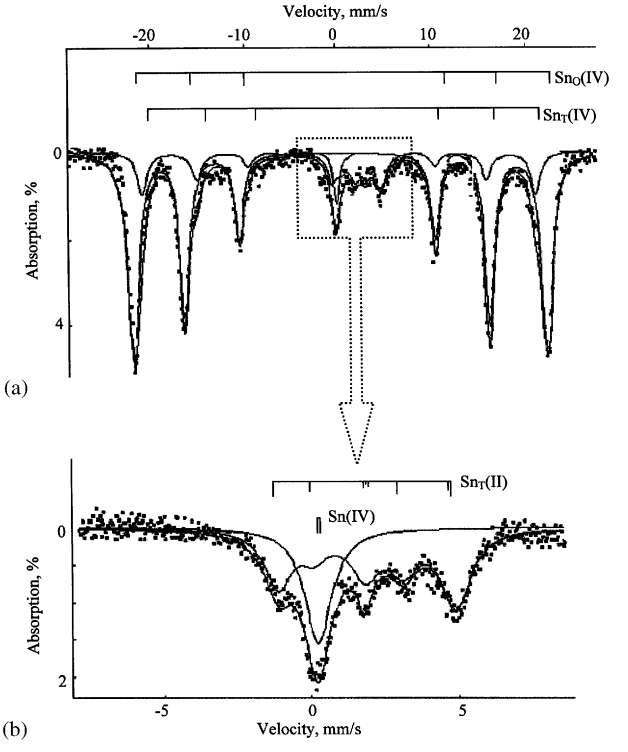

Fig. 6. (a–b) ^{119}Sn Mössbauer spectra of $Sr_2Fe_{1.98}Sn_{0.02}O_5$ (80 K) recorded in the different velocity ranges (see text).

Table 2
^{119}Sn Mössbauer parameters of "reduced" $Sr_2Fe_{1.98}Sn_{0.02}O_5$ ferrite (after heating in He-atmosphere) recorded at 80 K

Site	δ (mm/s) ± 0.01	$eQ_{3/2}V_{zz}/2$ (mm/s) ± 0.01	H (kOe) ± 1	φ ° ± 2	$\eta \pm 0.02$	θ° ± 2	A, % ± 1
Sn_O(IV)	0.20	−0.84	372	–	–	86	78
Sn_T(IV)	0.39	1.37	360	–	–	90	10
Sn_T(II)	2.40	1.87	34	3	0.5	89	12

in a small velocity range were carried out (Fig. 6b). The analysis of the spectrum was realized within the complete Hamiltonian $\hat{H}$ of combined electric and magnetic hyperfine interactions:

$$\hat{H} = -g\mu_N H\{I_z\cos\theta + (I_x\cos\varphi + I_y\sin\varphi)\sin\theta\} + eQV_{zz}/12\{3I_z^2 - 15/2 + \eta(I_x^2 - I_y^2)\},$$

where I_i $(i = z, x, y)$ are the components of the nucleus momentum of ^{119}Sn; θ $(0 \leqslant \theta \leqslant 180°)$ and φ $(0 \leqslant \varphi \leqslant 360°)$ are the orientation angles with respect to the principal axes of the EFG; $\eta = V_{xx} - V_{yy}/V_{zz}$ is asymmetry parameter; $|V_{zz}| > |V_{yy}| > |V_{xx}|$ are the components of the EFG. The resulting Mössbauer parameters are presented in Table 2.

The large positive isomer shift of additional absorption corresponds to divalent Sn^{2+} ions. It is noteworthy that the existence of spectra of the Sn^{2+} cations, measured in the magnetically ordered temperature range of $Sr_2Fe_{1.98}Sn_{0.02}O_5$, contain the magnetic Zeeman structure, which unambiguously indicates the stabilization of these ions in the studied ferrite lattice. Two examples of magnetically ordered compounds are known, where impurity tin ions were stabilized in a bivalent state: EuS:^{119}Sn [34] and MnS:^{119}Sn [35]. In both cases, the spectra of $^{119}Sn^{2+}$ are characterized by high positive isomer shifts, $\delta \approx 4$ mm/s, and by virtually zero quadrupole splitting, which shows the stabilization of the spherically symmetric Sn^{2+}:$5s^25p^0$ cations in octahedral sites of these sulfides.

In the case of $Sr_2Fe_{1.98}Sn_{0.02}O_5$, the spectrum of the Sn^{2+} cations has a smaller isomer shift, but much higher quadrupole splitting. In addition, the sign of the quadrupole coupling constant, $eQ_{3/2}V_{zz}$, determined from the spectrum is positive for Sn^{2+} sites. Since $Q_{3/2}(^{119}Sn) < 0$, this means that V_{zz} at divalent tin nucleus is also negative, in agreement with the observed sets of $|eQ_{3/2}V_{zz}|$ and δ values which imply a strong p_z-character (stereochemical activity) of the Sn^{2+} lone pair. Furthermore, the observed values of quadrupole splitting, $\Delta = eQ_{3/2}V_{zz}/2(1+\eta^2/3)^{1/2}$, and δ are close to those reported for tetragonal SnO modification ($\delta = 2.8$ mm/s, $\Delta = 1.6$ mm/s) where each tin atom lies out of the plane defined by its four oxygen neighbors [36]. Taking into account the close parameters of the spectra of the Sn^{2+} cations in the studied ferrite structures and the tetragonal SnO modification, one can assume that impurity Sn^{2+} ions are stabilized in the

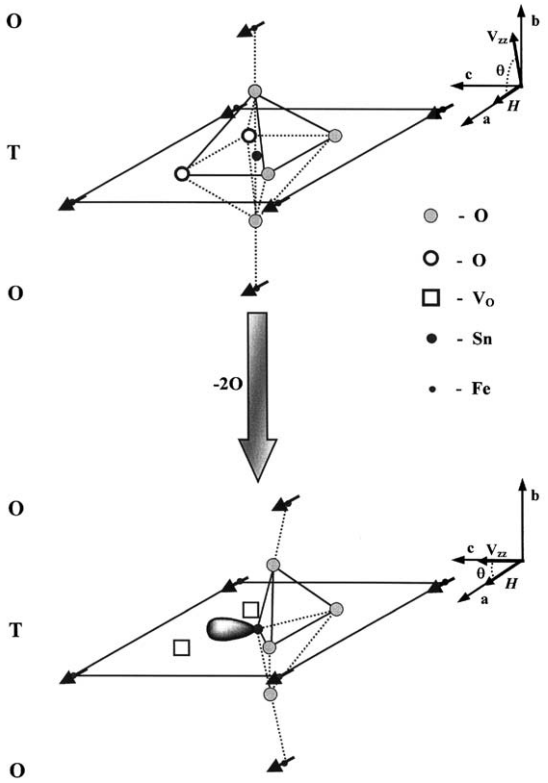

Fig. 7. Schematic representation of the change of ^{119}Sn local environment in the $Sr_2Fe_{1.98}Sn_{0.02}O_5$ structure upon the "reducing" heating in He-atmosphere.

sp^3d-hybrid state in the environment of the distorted teragonal pyramid. The angle $\theta \approx 90°$ determined from the spectra means that the hybrid orbital direction containing a stoichiometrically active lone Sn^{2+} pair perpendicular to the direction of the hyperfine magnetic field $H(Sn^{2+})$.

On the basis of the above Mössbauer spectra, we can propose a scheme (Fig. 7) of the processes leading to a structure change of the local environment of the "Sn_T^{4+}" cations at reduction annealing of $Sr_2Fe_{1.98}Sn_{0.02}O_5$ ferrite. According to Fig. 7, a fraction of the "Sn_T^{4+}" cations lose two neighborings oxygen anions during reduction to transit into a divalent state. Removing two oxygen atoms maintaining the octahedral coordination of "Sn_T^{4+}" cations, one sees the result in the localization of a lone Sn_T^{2+} electron pair along the direction (100) coinciding with the direction of magnetic moments of Fe_T^{3+} and Fe_O^{3+} cations inducing the hyperfine magnetic field $H(Sn^{2+})$.

Re-oxidation of $Sr_2Fe_{1.98}Sn_{0.02}O_5$ leads to total disappearance of the Sn_T^{2+} sub-spectrum with a simultaneous increase of contribution of the sub-spectrum corresponding to "Sn_T^{4+}". This result indicates chemical reversibility of the processes in the local environment of the "Sn_T^{4+}"/Sn^{2+} cations in the tetrahedral sublattice of the brownmillerite-type ferrite.

5. Conclusions

The hyperfine parameters and local structure of the ^{57}Fe and ^{119}Sn (probe) atoms in tin-doped $Sr_2Fe_{1.98}Sn_{0.02}O_5$ ferrite have been for the first time investigated. The ^{57}Fe Mössbauer spectra recorded at $T < T_N$ comprise two magnetic Zeeman sextets; by their δ and H values, these sub-spectra arise from the trivalent iron cations in the octahedral (Fe_O) and the tetrahedral (Fe_T) local oxygen environments. A large difference between both $\Delta\delta = 0.16$ mm/s and $\Delta H = 88$ kOe ($T = 80$ K) observed for Fe_O^{3+} and Fe_T^{3+} cations is interpreted as an indication of a greater covalence of the Fe_T–O chemical bonds in the Fe_TO_4 polyhedra. The observed ^{57}Fe hyperfine parameters are very close to those for $Sr_2Fe_2O_5$ ferrite.

The ^{119}Sn spectra recorded above and below the magnetic ordering temperature indicate that diamagnetic Sn^{4+} dopant ions are located in two non-equivalent sites. The observed values of the isomer shifts and lattice contributions to the EFG both tin sites were discussed supposing that Sn^{4+} cations substitute iron cations in the octahedral (Sn_O) and tetrahedral (Sn_T) sublattices. The analysis of the $H(Sn_O)$ and $H(Sn_T)$ values showed that Sn_T^{4+} ions, stabilized in the tetrahedral sublattice, complete their nearest anion surroundings up to the octahedral (Sn_TO_6) oxygen coordination ("Sn_T^{4+}"), which appears to be most typical for tetravalent tin atoms. It has been supposed that the different behavior of Sn^{4+} impurity ions in isostructural $Sr_2Fe_2O_5$ and $Ca_2Fe_2O_5$ ferrites can be related to different mechanisms of phase formation of these compounds.

The different changes induced in Sn_O^{4+} and "Sn_T^{4+}" sub-spectra by annealing of the simple $Sr_2Fe_{1.98}Sn_{0.02}O_5$ in a gas flux ($He + 2\%H_2$) are shown to reflect different local surrounding of both tin probe ions in the ferrite structure. It has been shown that annealing under He-atmosphere removes oxygen from the nearest anion surrounding of a fraction of the "Sn_T^{4+}" ions with formation of divalent Sn_T^{2+} sites. The parameters of combined electric and magnetic hyperfine interactions of the Sn_T^{2+} sub-spectrum indicate that five sp^3d tin orbitals form four bonds directed towards the O^{2-} ions and fifth non-bonding orbital (lone pair). Re-oxidation of the $Sr_2Fe_{1.98}Sn_{0.02}O_5$ leads to total disappearance of the Sn_T^{2+} sub-spectrum with a simultaneous increase of "Sn_T^{4+}" contribution and thus clearly demonstrates the chemical reversibility of the processes in the local environment of tin probe atoms.

Acknowledgments

We would like to thank Professor Jean Etourneau, for fruitful discussions. This work has been supported by Russian Foundation for Basic Research, grant No. 03-03-32662.

References

[1] Y. Takeda, K. Kanno, T. Takada, O. Yamamoto, M. Takano, N. Nakayama, Y. Bando, J. Solid State Chem. 63 (1986) 237.
[2] Y. Teraoka, H.-M. Zhang, S. Furukawa, N. Yamazoe, Chem. Lett. 11 (1985) 1743.
[3] T. Nakamura, M. Misona, Y. Yoneda, J. Catal. 83 (1983) 151.
[4] W. Göpel, Sensors Update 1 (1996) 47.
[5] V. Kozhevnikov, I. Leonidov, M. Patarkeev, E. Mitberg, J. Solid State Chem. 158 (2000) 320.
[6] V. Thangadurai, P. Schmid-Beurmann, W. Weppner, Mater. Res. Bull. 37 (2002) 599.
[7] V. Kharton, A. Kovalevsky, A. Viskup, J. Jurado, F. Figueiredo, E. Naumovich, J. Frade, J. Solid State Chem. 156 (2001) 437.
[8] M. Wyss, A. Reller, H.R. Oswald, Solid State Ionics 101–103 (1997) 547.
[9] M. Kim, H. Cho, C. Yo, J. Phys. Chem. Solids 59 (9) (1998) 1369.
[10] P. Schmid Beurmann, V. Thangadurai, W. Weppner, J. Solid State Chem. 174 (2003) 392.
[11] K. Roh, K. Ryu, C. Yo, J. Solid State Chem. 142 (1999) 288.
[12] P. Adler, S. Eriksson, Z. Anorg. Allg. Chem. 626 (2000) 118.
[13] J. Waerenborgh, F. Figueiredo, J. Frade, M. Colomer, J. Jurado, J. Phys.: Condens. Matter 13 (2001) 8171.
[14] I. Minyaylova, I. Presnyakov, K. Pokholok, A. Sobolev, A. Baranov, G. Demazeau, G. Govor, A. Vetcher, J. Solid State Chem. 151 (2000) 313.
[15] I. Presnyakov, K. Pokholok, I. Minyailova, V. Tkachenko, A. Sobolev, Russian J. Inorganic Chem. 43 (11) (1998) 1735.
[16] A. Moskvin, N. Ovanesyan, V. Trukhtanov, Hyperfine Interactions 5 (1977) 13.
[17] J. Linden, P. Karen, A. Kjekshus, J. Miettinen, M. Karppinens, J. Solid State Chem. 144 (1999) 398.
[18] M. Schmidt, S. Campbell, J. Solid State Chem. 156 (2001) 292.
[19] M. Takano, T. Okita, N. Nakayama, Y. Bando, Y. Takeda, O. Yamamoto, J. Goodenough, J. Solid State Chem. 73 (1988) 140.
[20] T.C. Gibb, J. Chem. Soc. Dalton Trans. 1985, 1455.
[21] F. Menil, J. Phys. Chem. Solids 46 (1985) 763.
[22] G. Le Caër, J. Dubois, L. Häggström, T. Ericsson, Nucl. Instrum. Methods 157 (1978) 127.
[23] P. Flinn, Mössbauer Isomer Shifts, North-Holland, Amsterdam, 1978.
[24] P. Fabritchnyi, L. Fournes, G. Demazeau, M. Afanasov, I. Presniakov, J. Solid State Chem. 96 (1992) 263.
[25] I. Bezverkhy, M. Afanasov, M. Danot, P. Fabritchnyi, Mater. Res. Bull. 35 (2000) 629.
[26] G. Demazeau, P. Fabritchnyi, L. Fournes, I. Presniakov, S. Darracq, V. Gorkov, K. Pokholok, J. Etourneau, Solid State Commun. 87 (1993) 109.
[27] I. Ljubutin, S. Vishnyakov, ZhETF 61 (1971) 1962.
[28] M. Takano, Y. Takeda, M. Shimada, T. Matsuzawa, T. Shinio, J. Phys. Soc. Japan 39 (1975) 656.

[29] S. Ichiba, T. Yamaguchi, Chem. Lett. 1984 1681.
[30] L. Beliaeve, I. Ljubutin, B. Mill', Russian J. Crystallogr. 15 (1970) 174.
[31] C. Greaves, A. Jacobson, B. Tofield, B. Fender, Acta Crystallogr. B 31 (1975) 641.
[32] I. Presniakov, K. Pokholok, I. Minyaylova, V. Tkachenko, A. Sobolev, Baranov, Izv. Akad. Nauk 63 (7) (1999) 1459.
[33] J. Hodges, S. Short, J. Jorgensen, X. Xiong, B. Dambrowski, S. Mini, C. Kimball, J. Solid State Chem. 151 (2000) 190.
[34] N. Bykovetz, Solid State Commun. 18 (1976) 143.
[35] M. Danot, V. Tkachenko, K. Pokholok, S. Maingaud, P. Fabritchnyi, J. Rouxel, Mater. Res. Bull. 30 (1995) 563.
[36] J. Boyle, D. Bunbury, C. Edwards, Proc. Phys. Soc. 79 (1962) 416.